ELSEVIER

International Journal of Pharmaceutics 192 (1999) 147–158

international journal of pharmaceutics

www.elsevier.com/locate/ijpharm

Synthesis and evaluation of *N*-acetylprolinate esters — novel skin penetration enhancers

Srini N. Tenjarla *[,1], Ram Kasina, Porranee Puranajoti, Mehboob S. Omar, Wayne T. Harris

Department of Pharmaceutical Sciences, Southern School of Pharmacy, Mercer University, 3001 Mercer University Drive, Atlanta, GA 30341, USA

Received 2 June 1998; received in revised form 1 June 1999; accepted 20 August 1999

Abstract

A series of *N*-acetylproline esters (alkyl side chain length, 5-18) were synthesized and tested for potential skin penetration enhancement activity using modified Franz diffusion cells and hairless mouse skin as the penetration barrier. Benazepril and hydrocortisone were used as model drugs and were applied as saturated solutions in propylene glycol. The enhancers were added at a concentration of 5% (w/v). Drug flux, permeability coefficient and enhancement ratios for permeability coefficient were determined. Azone was used as the positive control. While all the compounds tested increased the skin penetration of hydrocortisone, the 5- and 8- carbon esters had no significant effect on the skin penetration of benazepril. The highest fluxes were obtained with 11, 12, and 18-carbon esters and they were comparable to Azone. There was no significant difference between the fluxes obtained with 2 and 5% (w/v) concentrations of the 12-carbon ester on hydrocortisone permeation. The 16-carbon ester, where ethanol was used as a cosolvent, significantly increased the fluxes of both the drugs compared to the control. Differential scanning calorimetric studies suggested that the enhancers may be acting on the lipids of the stratum corneum and their effect was similar to that of Azone. The membrane/vehicle partition coefficient studies indicated an increase in benazepril partition coefficient with enhancer treatment compared to the control. Maximum flux increase was obtained with the 11 and 12 carbon (alkyl chain length) esters for both benazepril and hydrocortisone. The 18- carbon ester which has a cis-double bond in the alkyl side chain, also increased the flux significantly.

Keywords: Benazepril; Hydrocortisone; Penetration enhancer; *N*-acetylprolinate esters; Membrane/vehicle partition coefficient

1. Introduction

Transdermal delivery of drugs offers the advantages of prolonged action, better patient compliance, predictable drug concentrations in the blood, higher bioavailability and less toxicity

* Corresponding author. Tel: +1-205-5812581; fax: +1-205-5812888.

E-mail address: tenjarla@serquest.com (S.N. Tenjarla)

[1] Present address: Pharmaceutical Formulations, Southern Research Institute, 2000 Ninth Avenue South Birmingham, AL 35205, USA.

0378-5173/99/$ - see front matter
PII: S0378-5173(99)00300-2

(Franz et al., 1991). However, only few drugs are sufficiently permeable across the skin to provide the necessary blood concentrations to elicit the desired clinical response. This is due to the excellent barrier properties provided by the stratum corneum, the outermost layer of the skin, which is composed of keratin filled cells embedded in a lipid matrix (Walters, 1989). For most drugs the major route of skin penetration is believed to be through the lipid matrix (intercellular route). For increased penetration of any drug, the barrier function of the stratum corneum must be decreased either by disrupting the highly ordered structure of intercellular lipids or by interaction with intracellular protein components (Ghosh and Banga, 1993). This can be accomplished by using chemical skin penetration enhancers. Many compounds have been evaluated and shown to be effective enhancers. Previously, the 5-carbon ester, *n*-pentyl *N*-acetylprolinate (PNAP), was evaluated in human cadaver skin using benzoic acid (Harris et al., 1995), and in hairless mice skin using hydrocortisone (Fincher et al., 1996) as the model drugs. In this report, a number of other *N*-acetylproline esters were synthesized and tested as potential skin penetration enhancers using benazepril and hydrocortisone as model drugs. Benazepril is an ACE inhibitor indicated for the treatment of hypertension. It has a high water solubility and low oral bioavailability. Hydrocortisone is a relatively more lipophilic drug with low water solubility. The effect of *N*-acetylproline esters on skin penetration of these two model drugs was determined. Proline esters were used because pyrrolidone derivatives are known to increase the penetration of drugs through the skin (Sasaki et al., 1991).

Differential scanning calorimetry (DSC) has been widely used to investigate the effect of penetration enhancers on the lipid and protein components of stratum corneum (Van Duzee, 1975). DSC thermograms of the stratum corneum treated with fatty acids indicated that they affected the lipid transition and did not affect the protein transition (Francoeur et al., 1990). A similar effect was observed with Azone and alkyl sulfoxide (Goodmann and Barry, 1986). It was concluded from these studies that these enhancers acted by disrupting the lipid packing in the intercellular bilayers of stratum corneum. In this study, the effect of *N*-acetylprolinate esters on hairless mouse stratum corneum was evaluated by DSC studies.

Another approach to probe into the mechanism of penetration enhancement is to measure the solute partition coefficients by membrane vehicle partitioning studies. In the present study, a slight modification of the previously published study was used (Raykar et al., 1988).

2. Materials and methods

2.1. Materials

Benazepril was a generous gift from Novartis Pharmaceuticals, Suffern, NY. ^{3}H-hydrocortisone was purchased from Dupont NEN, Boston, MA. L-proline, *p*-toluenesulfonic acid hydrate, toluene, acetic anhydride, ethyl acetate, 1-pentanol, 1-octanol, 1-decanol, 1-undecanol, 1-dodecanol, 1-hexadecanol, and oleyl alcohol were purchased from Aldrich Chemical Company, Milwaukee, WI and were used without further purification. Hydrocortisone and all other chemicals were from Sigma Chemicals, St. Louis, MO.

2.2. Instrumentation

A Lambda 4B, Perkin-Elmer 400 UV-spectrophotometer was used for the UV spectrophotometric analysis. NMR and IR spectra were obtained with Gemini-300BB spectrophotometer and Perkin-Elmer 16 PC FT-IR spectrophotometer, respectively. Elemental analysis was performed by Atlantic Microlabs, Atlanta, GA. For ^{3}H-hydrocortisone, the amount of radioactivity permeated was monitored by Beckman LS 6500 liquid scintillation counter. Differential scanning calorimetry thermograms were obtained with Seiko DSC 220C differential scanning calorimeter.

2.3. Synthesis of N-acetylproline esters

The chemical structures of *N*-acetylproline and its esters are shown in Fig. 1. The synthesis of *N*-acetylproline and *n*-pentyl-*N*-acetylprolinate (PNAP) were reported earlier (Harris et al., 1995).

n-Octyl-*N*-acetylprolinate (ONAP): *N*-acetylproline (8.05 g, 0.051 mol), *n*-octanol (4.84 g, 0.037 mol), *p*-toluenesulfonic acid hydrate (0.97 g, 0.0051 mol), and toluene (100 ml) were placed in a 250-ml round-bottomed flask fitted with Dean-Stark trap, reflux condenser, and a magnetic stirrer. The reaction mixture was refluxed for approximately 2 h, until no further separation of water was observed. The volatile material was then removed by distillation at atmospheric pressure to give a yellow residue. The crude product was purified by vacuum distillation which yielded a colorless oil (7.61 g, 76%), bp 140-145°C/0.1 mmHg; ^{1}H NMR ($CDCl_3$): δ 0.8 (3H, t), 1.2 (12H, m), 1.8-2.2 (4H, m), 2.0 (3H, s), 3.5 (1H, m), 3.6 (1H, m), 4.0 (2H, m), and 4.3, 4.4 (1H, dd); IR (film): 2856.6 (CH stretching), 1746.7, 1659.2 cm^{-1} (carbonyl).

n-Decyl-*N*-acetylprolinate (DNAP): *N*-acetylproline (8.05 g, 0.051 mol), *n*-decanol (5.89 g, 0.037 mol), *p*-toluenesulfonic acid hydrate (0.97 g, 0.0051 mol), and toluene (100 ml) were placed in a 250-ml round-bottomed flask fitted with Dean-Stark trap, reflux condenser, and a magnetic stirrer. The reaction mixture was refluxed for approximately 2 h, until no further separation of water was observed. The volatile material was then removed by distillation at atmospheric pressure to give a yellow residue. The crude product was purified by vacuum distillation which yielded a colorless oil (7.92 g, 71.6%), bp 142-145°C/0.1 mmHg; ^{1}H NMR ($CDCl_3$): δ 0.8 (3H, t), 1.3 (16H, m), 1.8-2.2 (4H, m), 2.0 (3H, s), 3.5 (1H, m), 3.6(1H, m), 4.0 (2H, m), and 4.3, 4.4 (1H, dd); IR (film): 2856.6 (CH stretching), 1751.3, 1663.8 cm^{-1} (carbonyl).

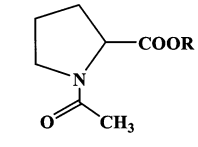

N-acetylprolinate

Compound	R
PNAP	$-C_5H_{11}$
ONAP	$-C_8H_{17}$
DNAP	$-C_{10}H_{21}$
UNAP	$-C_{11}H_{23}$
DDNAP	$-C_{12}H_{25}$
HDNAP	$-C_{16}H_{33}$
Oleyl-NAP	$-C_{18}H_{35}$

Fig. 1. Chemical structures of *N*-acetylprolinate esters.

n-Undecyl-*N*-acetylprolinate (UNAP): *N*-acetylproline (8.05 g, 0.051 mol), *n*-undecanol (6.41 g, 0.037 mol), *p*-toluenesulfonic acid hydrate (0.97 g, 0.0051 mol), and toluene (100 ml) were placed in a 250-ml round-bottomed flask fitted with Dean-Stark trap, reflux condenser, and a magnetic stirrer. The reaction mixture was refluxed for ≈2 h, until no further separation of water was observed. The volatile material was then removed by distillation at atmospheric pressure to give a yellow residue. The crude product was purified by vacuum distillation which yielded a colorless oil (9.27 g, 80%), bp 167-170°C/0.1 mmHg; ^{1}H NMR ($CDCl_3$): δ 0.8 (3H, t), 1.4 (18H, m), 1.8-2.2 (4H, m), 2.0 (3H, s), 3.5 (1H, m), 3.6 (1H, m), 4.0 (2H, m), and 4.3, 4.4 (1H, dd); IR (film): 2854.0 (CH stretching), 1744.0, 1658.0 cm^{-1} (carbonyl).

n-Dodecyl-*N*-acetylprolinate (DDNAP): *N*-acetylproline (8.05 g, 0.051 mol), *n*-dodecanol (6.93 g, 0.037 mol), *p*-toluenesulfonic acid hydrate (0.97 g, 0.0051 mol), and toluene (100 ml) were placed in a 250-ml round-bottomed flask fitted with Dean-Stark trap, reflux condenser, and a magnetic stirrer. The reaction mixture was refluxed for ≈2 h, until no further separation of water was observed. The volatile material was then removed by distillation at atmospheric pressure to give a yellow residue. The crude product was purified by vaccum distillation which yielded a colorless oil (8.60 g, 71%), bp 205-208°C/0.1 mmHg; ^{1}H NMR ($CDCl_3$): δ 0.8 (3H, t), 1.4 (20H, m), 1.8-2.2 (4H, m), 2.0 (3H, s), 3.5 (1H, m), 3.6 (1H,m), 4.0 (2H, m), and 4.3, 4.4 (1H, dd); IR (film): 2854.0 (CH stretching), 1744.0, 1658.0 cm^{-1} (carbonyl).

n-Hexadecyl-*N*-acetylprolinate (HDNAP): *N*-acetylproline (5.08 g, 0.032 mol), 1-hexadecanol (7.74 g, 0.032 mol), *p*-toluenesulfonic acid hydrate (0.3 g, 0.0016 mol), and toluene (100 ml) were

placed in a 250-ml round-bottomed flask fitted with Dean-Stark trap, reflux condenser, and a magnetic stirrer. The reaction mixture was refluxed for ≈ 2 h, until no further separation of water was observed. The mixture was allowed to cool to room temperature and it was extracted consecutively, with 50 ml of 10% aqueous sodium bicarbonate and 50 ml of water. The organic layer was then dried, filtered and evaporated to give yellow oil. This oil was then placed on a short pad of silica gel and eluted with ethyl acetate–hexane (30:70) mixture to remove non-polar impurities. The product was obtained by elution with 300 ml of ethyl acetate followed by evaporation to give a yellow oil, which solidified on standing at room temperature (10.27 g, 84%), mp 45–47°C; ^{1}H NMR ($CDCl_3$): δ 0.8 (3H, t), 1.4 (28H, m), 1.8-2.2 (4H, m), 2.0 (3H, s), 3.5 (1H, m), 3.6 (1H, m), 4.0 (2H, m), and 4.3, 4.4 (1H, dd); IR (film): 2854.0 (CH stretching), 1738.0, 1636.0 cm^{-1} (carbonyl).

9-Octadecenyl-*N*-acetylprolinate (oleyl-NAP): *N*-acetylproline (8.05 g, 0.051 mol), oleyl alcohol (9.98 g, 0.037 mol), *p*-toluenesulfonic acid hydrate (0.97 g, 0.0051 mol), and toluene (100 ml) were placed in a 250-ml round-bottomed flask fitted with Dean-Stark trap, reflux condenser, and a magnetic stirrer. The reaction mixture was refluxed for ≈ 2 h, until no further separation of water was observed. The volatile material was then removed by distillation at atmospheric pressure to give a yellow residue. The crude product was purified by vacuum distillation which yielded a yellow oil (7.88 g, 52%), bp 192-196°C/0.1 mmHg; ^{1}H NMR ($CDCl_3$): δ 0.8 (3H, t), 1.4 (24H, m), 1.8-2.2 (8H, m), 2.0 (3H, s), 3.5 (1H, m), 3.6 (1H, m), 4.0 (2H, m), 4.3, 4.4 (1H, dd) and 5.3 (2H, m); IR (film): 2854.0 (CH stretching), 1744.0, 1654.0 (carbonyl), 3000 cm^{-1} (olefinic-CH).

2.4. Analytical methods

A sensitive HPLC assay was developed for the analysis of benazepril in the skin diffusate samples. HPLC assay was performed using reversed phase C-18 Spherisorb ODS2 column (4×250 mm), Alcott 738 Autosampler, LDC Analytical ConstaMetric III pump, LDC Analytical SpectroMonitor 3100 equipped with UV detector, and Hewlett Packard P3394A integrator. The mobile phase used was 30% acetonitrile in phosphate buffer (pH 5.4). The flow rate was 1.5 ml/min and the effluent was monitored at 238 nm. The within day and between day variations of the slopes of the standard curves were determined. Tritiated hydrocortisone content was determined by a Beckman LS 6500 liquid scintillation counter.

2.5. Skin permeation experiments

Hairless mice (SKH:SR-1), 8-14 weeks old, were purchased from Charles River Laboratories, Wilmington, MA. The animals were euthanized with carbon dioxide. A portion of the full thickness abdominal skin was carefully excised. The dermal side of the skin was carefully cleared of any adhering subcutaneous tissues and blood vessels. The skin was mounted on modified Franz diffusion cells. 150 μl of saturated benazepril or hydrocortisone solution in propylene glycol (with or without 5% w/v of *N*-acetylproline ester) was added to the top of the skin in the donor chamber. In case of hydrocortisone, a known amount of radioactivity (^{3}H-hydrocortisone) was also added to the test solution. The donor chamber and the sample port were occluded with Parafilm. Isotonic phosphate buffer (pH 7.4) was used as the receptor medium (receptor volume 10 ml) and the receptor chamber was maintained at 37 ± 1°C. 200 μl of receptor samples were taken at 1, 3, 5, 7, 9, 12, 15, 19, and 24 h and analyzed for benazepril by the developed HPLC assay. Tritiated hydrocortisone was monitored in the samples with a liquid scintillation counter and the total amount of steroid was determined using the cold to hot drug ratio. The removed sample was replaced with an equal volume of the buffer solution to maintain the contact between the buffer and the skin. Analysis of each sample was corrected for previously removed volume to represent cumulative drug amount permeated for each sampling time.

2.5.1. Data analysis

The cumulative amount of drug permeated across the skin was plotted against time. The

steady state flux (J) was calculated from the slope of the linear region of the above plot. The lag time (T) was calculated by extrapolating the linear region of the curve to the X-axis. Permeability coefficient (Kp) was calculated from the ratio of flux to drug concentration in the donor chamber. Enhancement ratios for Kp (ERKp) were calculated by dividing the Kp after enhancer treatment with Kp for the control. All data were represented as mean $\pm$ S.D. One way analysis of variance (ANOVA) was used to test for significance. The Bonferroni test for comparison of means (post-hoc test) was performed to compare the means within different groups. A probability of $p < 0.05$ was considered statistically significant.

2.6. Differential scanning calorimetric (DSC) studies

The effect of the N-acetylprolinate esters on hairless mouse stratum corneum was studied with a Seiko DSC 220C differential scanning calorimeter. The hairless mouse stratum corneum samples (average 20 mg/sample) were treated with the esters for 24 h. They were scanned at the rate of 5°C/min over 25 to 125°C temperature range and thermograms were obtained. Azone was used as the positive control. The changes in the endotherms indicate how the enhancers modify phase transitions within the stratum corneum.

2.7. Membrane/vehicle partition studies

The membrane–vehicle partition studies were conducted with full thickness hairless mouse skin. The measured values were corrected for the contribution from viable epidermis–dermis, which is ≈ 95 wt% of full thickness skin. This correction was made assuming the partition coefficient of unity for the whole thickness skin, and calculating the partition coefficient for the stratum corneum using the weight fraction of 0.05%. Known volumes (2 ml) of aqueous solutions of benazepril in pH 7.4 phosphate buffer were placed in screw-cap glass vials and maintained at 37°C in a water bath for equilibration. An aliquot from each vial was analyzed by HPLC to obtain the initial concentration of benazepril ($Ca_{(before)}$) in the bathing solution. Control hairless mice skin samples were treated with 200 μl of propylene glycol for 24 h. After 24 h, they were gently blotted, accurately weighed and placed in the vials with the drug solution. The vials were capped and placed in a water bath at 37°C with occasional gentle agitation for 48 h. The hydrated skin samples were then removed, blotted gently, and the solute concentrations ($Ca_{(after)}$) in the bathing solution were measured by HPLC.

The membrane–vehicle partition coefficients for the enhancer treated skin samples were also determined in a similar fashion. UNAP and PNAP were chosen for these studies. Azone was used as the positive control. Hairless mice skin samples were pretreated with 200 μl of 5% w/v of PNAP, or 5% w/v of UNAP, or 3% w/v of Azone in propylene glycol for 24 h. After 24 h, they were gently blotted, accurately weighed and placed in each vial. The vials were capped and placed in a water bath at 37°C with occasional gentle agitation for 48 h. The hydrated skin samples were then removed, blotted gently, and the solute concentrations in the bathing solution were measured by HPLC. The membrane–vehicle partition coefficient of the drug for the control and enhancer treated skin was calculated using the following equation:

$$\text{membrane/vehicle partition coefficient} = \frac{[Ca_{(\text{before})} - Ca_{(\text{after})}] * Wa * 0.05}{Ca_{(\text{after})} * Ws}$$

where: Wa, weight of the aqueous phase (mg); Ws, weight of the skin (mg).

3. Results and discussion

3.1. Characterization of N-acetylprolinate esters

The results of the elemental analysis of the synthesized N-acetylprolinate esters are shown in Table 1. The difference between the theoretical and actually found values was less than 0.4%. Their structures were further confirmed by FTIR and NMR spectroscopic studies, as reported in the methodology section.

Table 1
Elemental analysis results of *N*-acetylproline esters

N-acetylprolinate ester	Carbon (%) theoretical/actual	Hydrogen (%) theoretical/actual	Nitrogen (%) theoretical/actual
PNAP	63.41/63.51	9.31/9.41	6.16/6.08
ONAP	66.88/66.81	10.10/10.03	5.20/5.11
DNAP	68.65/68.46	10.50/10.41	4.71/4.69
UNAP	69.41/69.50	10.68/10.69	4.50/4.44
DDNAP	70.11/69.93	10.84/10.73	4.30/4.23
HDNAP	72.39/72.35	11.36/11.26	3.67/3.74
Oleyl-NAP	73.66/73.02	11.13/11.13	3.44/3.37

3.2. Analytical methods

Base line resolution for benazepril was attained with a retention time of 5.5 min under the test conditions. The within and between day coefficient variation of the slopes of the calibration curves was $<4\%$. The counting efficiency for the tritiated hydrocortisone was $>90\%$ and there was no quenching or chemi-luminescence due to the diffusion medium.

3.3. Skin permeation studies

3.3.1. Benazepril

The skin permeation parameters for benazepril were summarized in Table 2 and the permeation profiles are shown in Figs. 2 and 3. The mean flux of benazepril through control hairless mouse skin was 10.9 μg/cm^2 h. There was no significant increase in flux with PNAP and ONAP compared to the control. However, there was a significant increase in flux with all the other enhancers tested compared to the control. There was no significant difference in the lag time with the enhancer treatment. An increase in flux was in good correlation with an increase in *Km* and *Kp* values. However, there were no significant differences in D/d^2 values with enhancers compared to the control. This would be expected because *D* was dependent on the lag time, *T*, which was fairly constant. In our calculations, the diffusion coefficient was calculated from lag time '*T*' $\{(D/d^2 = 1/(6T)\}$. It must be pointed out that the assumption made here was that '*T*' is the diffusional lag time, which may not be the case for the heterogeneous and multilayer skin membrane.

As HDNAP was not soluble in propylene glycol, 0.053% (v/v) of ethanol was used as a cosolvent to dissolve HDNAP. Hence a different control was used for this group (with the same amount of ethanol). The skin permeation parameters were shown in Table 3. A significant increase in flux, *Kp*, *Km*, and *D* values and a significant decrease in lag time were observed with HDNAP treatment compared to the control. There was a 6.1-fold increase in ER (*Kp*). The rank order for *Kp* enhancement ratio was as follows: azone = oleyl NAP = UNAP > DDNAP > HDNAP > DNAP > ONAP = PNAP = control.

3.3.2. Hydrocortisone

The permeation parameters for hydrocortisone were summarized in Table 4 and the permeation

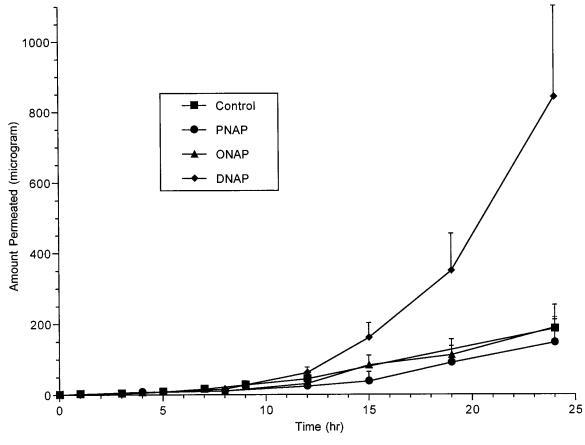

Fig. 2. Effect of 5% w/v of PNAP, ONAP and DNAP on benazepril permeation (mean ± S.D.) through hairless mouse skin ($n = 5$).

Table 2
Skin permeation parameters of benazepril through hairless mouse skin[a]

Enhancer	Flux (J) μg/cm^2 h	Lag time (T) h	Permeability coefficient (Kp) cm/h $\times 10^{-5}$	Partition coefficient ($Km*d$) cm $\times 10^{-3}$	Diffusion coefficient (D/d^2) /h $\times 10^{-3}$	ER (Kp)
Control	10.9 ± 1.8	8.4 ± 1.2	3.0 ± 0.5	1.6 ± 0.3	20.0 ± 2.8	1.0
With 5% w/v of PNAP	12.6 ± 0.8	9.1 ± 4.7	3.5 ± 0.2	2.5 ± 0.2	18.3 ± 9.6	1.2
With 5% w/v of ONAP	13.4 ± 5.4	9.4 ± 1.6	2.9 ± 1.2	1.7 ± 0.9	18.2 ± 3.2	1.0
With 5% w/v of DNAP	41.5* ± 15.1	10.5 ± 0.7	13.6* ± 4.9	8.7* ± 3.7	15.9 ± 1.0	4.5*
With 5% w/v of UNAP	430.2* ± 72.2	12.0 ± 1.1	120.2* ± 20.2	86.0* ± 13.6	14.0 ± 1.3	40.1*
With 5% w/v of DDNAP	217.3* ± 68.2	10.8 ± 1.2	71.1* ± 22.3	45.8* ± 13.5	15.6 ± 1.5	23.7*
With 5% w/v of oleyl-NAP	371.9* ± 134.8	8.1 ± 2.2	121.7* ± 44.1	56.4* ± 15.2	22.1 ± 5.6	40.6*
With 3% w/v of Azone®	500.6* ± 89.0	11.0 ± 2.0	203.0* ± 36.1	131.9* ± 24.9	15.7 ± 3.0	67.7*

[a] Data are presented as mean ± S.D. for each group ($n = 5$). Statistically significant ($P < 0.05$) from the control group.

Table 3
Effect of HDNAP on benazepril and hydrocortisone permeation through hairless mouse skin[a]

Benazepril	Flux (J) μg/cm^2 h	Lag time (T) h	Permeability coefficient (Kp) cm/h $\times 10^{-5}$	Partition coefficient (Km*d) cm $\times 10^{-3}$	Diffusion coefficient (D/d^2) /h $\times 10^{-3}$	ER (Kp)
Benazepril						
Control (with ethanol)	82.8 ± 12.0	12.9 ± 0.9	27.1 ± 3.9	21.1 ± 3.8	12.9 ± 0.9	1.0
With 5% w/v of HDNAP + 0.053% v/v of ethanol	$501.2^{b} \pm 119.6$	$6.7^{b} \pm 1.2$	$164.0^{b} \pm 39.1$	$63.7^{b} \pm 7.6$	$25.5^{b} \pm 4.6$	6.1^{b}
Hydrocortisone						
Control (with ethanol)	3.6 ± 1.8	5.7 ± 2.1	33.1 ± 17.3	13.3 ± 1.0	34.8 ± 17.3	1.0
With 5% w/v of HDNAP + 0.053% v/v of ethanol	$50.3^{b} \pm 8.7$	$2.0^{b} \pm 1.3$	$457.1^{b} \pm 79.2$	$54.1^{b} \pm 35.0$	$128.2^{b} \pm 71.2$	13.8^{b}

[a] Data are presented as mean $\pm$ S.D. for each group ($n = 6$).
[b] Statistically significant ($P < 0.05$) from the control group.

Table 4
Effect of *N*-acetylprolinate esters on hydrocortisone permeation through hairless mouse skin[a]

Enhancer	Flux (J) μg/cm^2 h	Lag time (T) h	Permeability coefficient (Kp) cm/h $\times 10^{-5}$	Partition coefficient ($Km*d$) cm $\times 10^{-3}$	Diffusion coefficient (D/d^2) /h $\times 10^{-3}$	ER (Kp)
Control	2.7 ± 1.1	13.0 ± 0.5	24.6 ± 5.8	19.4 ± 4.9	12.1 ± 0.5	1.0
With 5% w/v of PNAP[c]	$38.9^{d} \pm 16.9$	$7.2^{d} \pm 0.7$	$354.0^{d} \pm 153.8$	$148.5^{d} \pm 55.3$	$23.5^{d} \pm 2.5$	14.4^{d}
With 5% w/v of ONAP[c]	$47.8^{d} \pm 11.7$	11.1 ± 0.4	$434.7^{d} \pm 106.3$	$290.3^{d} \pm 70.3$	15.0 ± 0.5	17.7^{d}
With 5% w/v of DNAP[b]	$49.3^{d} \pm 11.6$	$4.9^{d} \pm 0.7$	$448.1^{d} \pm 105.1$	$128.1^{d} \pm 16.0$	$34.6^{d} \pm 4.7$	18.2^{d}
With 5% w/v of UNAP[c]	$82.7^{d} \pm 38.5$	$3.4^{d} \pm 1.6$	$751.9^{d} \pm 349.6$	$129.9^{d} \pm 22.1$	$59.2^{d} \pm 27.5$	30.6^{d}
With 5% w/v of DDNAP	$92.7^{d} \pm 13.3$	$3.3^{d} \pm 0.9$	$843.0^{d} \pm 120.9$	$164.1^{d} \pm 34.4$	$53.4^{d} \pm 12.6$	34.3^{d}
With 5% w/v of oleyl-NAP	$73.3^{d} \pm 16.7$	$1.1^{d} \pm 0.4$	$644.4^{d} \pm 152.1$	$41.5^{d} \pm 14.9$	$179.0^{d} \pm 74.7$	27.1^{d}
With 3% w/v of Azone®	$59.6^{d} \pm 11.1$	$2.3^{d} \pm 0.7$	$541.9^{d} \pm 100.6$	$71.4^{d} \pm 18.4$	$83.5^{d} \pm 40.1$	22.0^{d}

[a] Data are presented as mean $\pm$ S.D. for each group.
[b] $n = 6$.
[c] $n = 5$; and $n = 7$ for all other groups.
[d] Statistically significant ($P < 0.05$) from the control group.

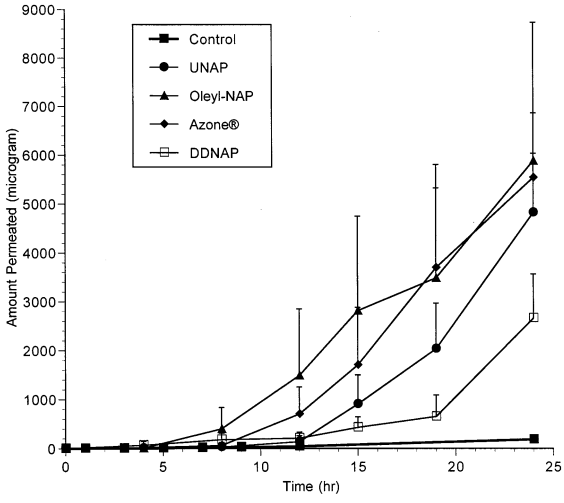

Fig. 3. Effect of 5% w/v of UNAP, DDNAP, Oleyl-NAP and 3% w/v of Azone® on benazepril permeation (mean ± S.D.) through hairless mouse skin ($n = 5$).

profiles were shown in Figs. 4 and 5. The mean steroid flux from control hairless mouse skin was 2.7 μg/cm^2 h. There was a significant increase in flux with all the enhancers tested compared to the control. This was in contrast with benazepril, where PNAP and ONAP had no significant enhancing effect. Since hydrocortisone has a low

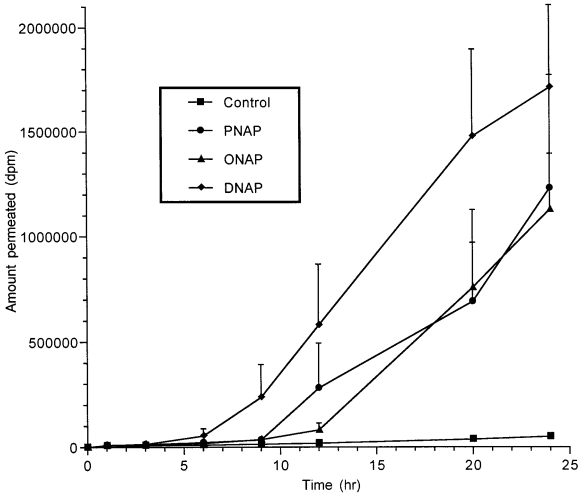

Fig. 4. Effect of 5% w/v of PNAP ($n = 5$), ONAP ($n = 5$), and DNAP ($n = 6$) on hydrocortisone permeation (mean ± S.D.) through hairless mouse skin.

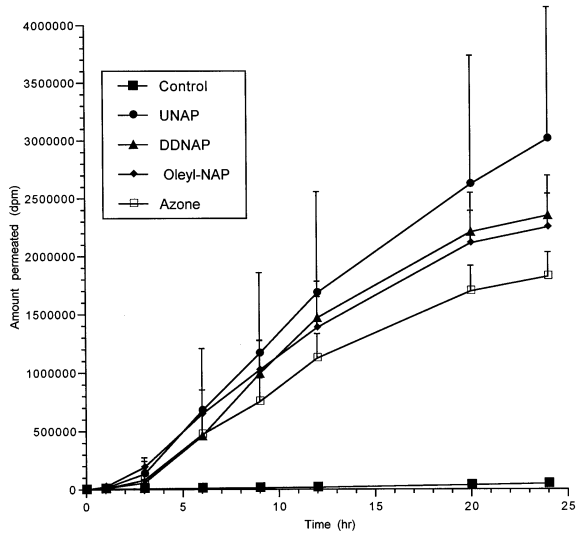

Fig. 5. Effect of 5% w/v of UNAP ($n = 5$), DDNAP ($n = 7$), Oleyl-NAP ($n = 7$) and 3% w/v of Azone® ($n = 7$) on hydrocortisone permeation (mean ± S.D.) through hairless mouse skin.

intrinsic permeation rate, it is expected that even a small change caused by enhancers would produce a significant increase in hydrocortisone permeation. On the other hand, benazepril has more balanced partitioning properties and has a relatively high intrinsic permeation rate. Hence, any small effect caused by PNAP and ONAP might not have contributed significantly to an increase in benazepril permeation. The highest fluxes were obtained with UNAP (82.7 μg/cm^2 h) and DDNAP (92.7 μg/cm^2 h). The flux obtained with the positive control, Azone, was 59.6 μg/cm^2 h. A significant increase in Km, and Kp values was observed with all the enhancers. A significant increase in D values and a significant decrease in lag time were also observed with all the enhancers (except ONAP). The increase in flux with ONAP appeared to be due to the increase in Km value compared to the control.

As reported before, ethanol was used as a co-solvent for HDNAP due to its limited solubility in propylene glycol and the appropriate control was used. The skin permeation parameters are shown in Table 3. A significant increase in flux, *Kp*, *Km*, and D values and a significant decrease in lag time were observed with HDNAP treatment compared

to the control. There was a 13.8-fold increase in ER (*Kp*) of hydrocortisone for the enhancer treated skin. The rank order for *Kp* enhancement ratio is as follows: DDNAP = UNAP > oleyl-NAP > azone > DNAP = ONAP = PNAP = HDNAP > control.

3.3.3. Effect of enhancer concentration

A 2% w/v of DDNAP was also tested to study the effect of enhancer concentration on hydrocortisone permeation. The flux obtained with 2% w/v of DDNAP was 93.8 ± 29.4 μg/cm^2 h. The corresponding *T*, *Kp*, *Km*d*, D/d^2, and ER-*Kp* values were 7.8 ± 1.1 h, 853.2 ± 267.7 ($\times 10^{-5}$) cm/h, 409.5 ± 172.2 ($\times 10^{-3}$) cm, $21.9 \pm 3.4 \times (10^{-3})$/h, and 34.7, respectively. There was no significant difference in flux, *Kp*, and ER-*Kp* values obtained with 2% and 5% w/v of enhancer concentrations. This suggests that a 2% w/v of enhancer concentration was sufficient to produce the observed enhancement activity. However, a significant increase in the lag time observed with 2% w/v enhancer.

3.3.4. Carbon chain length versus enhancement effect

A plot of ER-Kp versus carbon chain length for benazepril and hydrocortisone were shown in Figs. 6 and 7, respectively. All compounds were effective as skin penetration enhancers for hydrocortisone. The highest fluxes were obtained with alkyl chain length of 11-12 carbons for both hydrocortisone and benazepril. However, only compounds with alkyl chain length of 10 or greater were effective as enhancers for benazepril. The pentyl and octyl esters did not show any penetration enhancement for benazepril. The compounds, 11-carbon ester (UNAP) and 12-carbon ester (DDNAP), possess both hydrophilic and lipophilic components similar to Azone which might have contributed to increased penetration through the skin similar to Azone. This is also in agreement with the literature, where, for other penetration enhancers like fatty acids and alcohols, maximum enhancement ratios were obtained with alkyl chain length of 10-12 (Cooper et al., 1985; Aungst et al., 1986). High enhancement ratio for *Kp* was also observed with 18- carbon ester (oleyl-NAP). This was attributed to the presence of a cis-double bond which introduces a kink in the alkyl side chain. This can affect the mode of packing of these enhancer molecules into the lipid matrices of stratum corneum (Cooper, 1984).

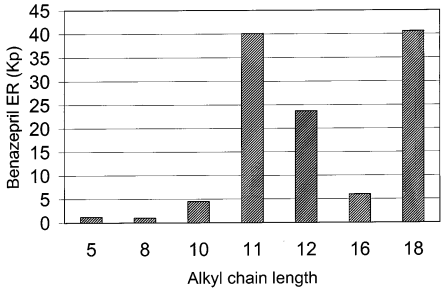

Fig. 6. Enhancement ratios (ER-Kp) versus alkyl chain length of *N*-acetylprolinate esters on benazepril permeation through hairless mouse skin.

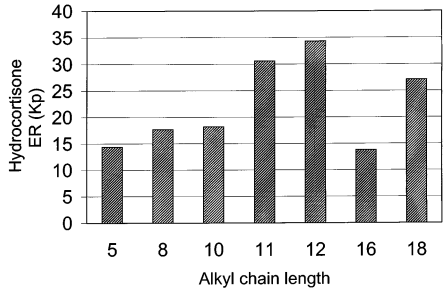

Fig. 7. Enhancement ratios for (ER-Kp) versus alkyl chain length of *N*-acetylprolinate esters on hydrocortisone permeation through hairless mouse skin.

3.4. Differential scanning calorimetric studies

In the control hairless mouse stratum corneum sample, three transitions were identified. The transitions at 48.8 and 71.7°C were attributed to lipid melting and the higher transition at 99.4°C was assigned to protein denaturation. The effects of UNAP, DDNAP, oleyl-NAP and Azone on these three transitions were studied.

The UNAP pretreatment decreased the lower lipid transition from 48.8 to 47.8°C and eliminated the higher lipid transition at 71.7°C. When the stratum corneum was treated with DDNAP, oleyl-NAP, and Azone, both the lipid transitions

at 48.8 and 71.7°C disappeared. From these observations, it may be concluded that DDNAP, oleyl-NAP, and Azone appear to act in similar manner by eliminating the lipid transitions. As UNAP eliminated only one lipid transition and decreased the other lipid transition, it may be acting by a similar mechanism with a less significant effect on stratum corneum lipids compared to other enhancers. In general, it appears that the enhancers had some effect on the lipid transitions of the stratum corneum.

3.5. Membrane/vehicle partitioning studies

The control membrane/vehicle partition coefficient of benazepril in hairless mouse skin was found to be 0.77 ± 0.25 The membrane/vehicle partition coefficient for PNAP treated skin was 0.87 ± 0.28 and there was no significant difference between the partition coefficients of control and PNAP treated skin. Significant differences in partition coefficients were observed with UNAP (1.6 ± 0.28) and Azone (2.46 ± 0.34) pre-treatment compared to that of control. However, there was no significant difference observed between pretreatment with UNAP, and with Azone.

From these observations, it was concluded that the UNAP and Azone significantly increased the partition coefficient of benazepril and thereby increased the drug partitioning into the skin. This may be one of the reasons for the higher ER (Kp) of benazepril with UNAP and Azone, in the skin permeation studies. The fact that the PNAP pretreatment did not significantly increase the membrane/vehicle partition coefficient, was in agreement with its lower enhancement activity compared to the other *N*-acetylprolinate esters. In summary, novel skin penetration enhancers were synthesized which showed penetration enhancement for both hydrophilic and hydrophobic drugs.

Acknowledgements

The authors gratefully acknowledge Novartis Pharmaceutical, Suffern, NY for benazepril. and Dr T.K. Mandal, Xavier University of Louisiana, New Orleans, LA and Dr I. Haruna, Clark Atlanta University, Atlanta, GA for their analytical support.

References

Aungst, B.J., Rogers, N.J., Shefter, E., 1986. Enhancement of naloxone penetration through human skin in vitro using fatty acids, fatty alcohols, surfactants, sulfoxides, and amides. Int. J. Pharm. 33, 225–234.

Cooper, E.R., 1984. Increased skin permeability for lipophilic molecules. J. Pharm. Sci. 73, 1153–1156.

Cooper, E.R., Merritt, E.W., Smith, R.L., 1985. Effect of fatty acids and alcohols on the penetration of acyclovir across human skin in vitro. J. Pharm. Sci. 74, 688–689.

Fincher, T.K., Yoo, S.D., Player, M.R., Sowell, J.W. Sr., Michniak, B.B., 1996. In vitro evaluation of a series of *N*-dodecanoyl-L-amino acid methyl esters as dermal penetration enhancers. J. Pharm. Sci. 85, 920–923.

Francoeur, M.L., Golden, G.M., Potts, R.O., 1990. Oleic acid: its effects on SC in relation to (trans) dermal drug delivery. Pharm. Res. 7, 621.

Franz, T.J., Tojo, K., Shah, K.R., Kydonieus, A., 1991. Transdermal delivery. In: Kydonieus, A. (Ed.), Treatise on Controlled Drug Delivery: Fundamentals, Optimization, Applications. Marcel Dekker, New York, pp. 341–345.

Ghosh, T.K., Banga, A.K., 1993. Methods of enhancement of transdermal drug delivery: part IIA, chemical penetration enhancers. Pharm. Tech. 17 (4), 62–90.

Goodmann, M., Barry, B.W., 1986. Action of skin penetration enhancers, Azone, oleic acid, and DMSO: permeation and DSC studies. J. Pharm. Pharmacol. 38, 71.

Harris, W.T., Tenjarla, S.N., Holbrook, J.M., Smith, J., Mead, C., Entrekin, J., 1995. *N*-pentyl *N*-acetylprolinate. A new skin penetration enhancer. J. Pharm. Sci. 84, 640–642.

Raykar, P.V., Man-Cheong, Fung., Anderson, B.D., 1988. The role of protein and lipid domains in the uptake of solutes by human SC. Pharm. Res. 5 (3), 140–150.

Sasaki, H., Kojima, M., Mori, Y., Nakamura, J., Shibasaki, J., 1991. Enhancing effect of pyrrolidone derivatives on transdermal penetration of 5-fluorouracil, triamcinolone acetonide, indomethacin and flurbiprofen. J. Pharm. Sci. 80, 533–538.

Van Duzee, B.F., 1975. Thermal analysis of human SC. J. Invest. Dermatol. 65, 404.

Walters, K.A., 1989. Penetration enhancers and their use in transdermal therapeutic systems. In: Hadgraft, J., Guy, R.H. (Eds.), Transdermal Drug Delivery: Developmental Issues and Research Initiatives. Marcel Dekker, New York, pp. 198–201.